Renner–Teller splitting in the C 1s→π * excited states of CS 2 , OCS, and CO 2

Jun-ichi Adachi, Nobuhiro Kosugi, Eiji Shigemasa, and Akira Yagishita

Citation: The Journal of Chemical Physics **107**, 4919 (1997); doi: 10.1063/1.474855
View online: http://dx.doi.org/10.1063/1.474855
View Table of Contents: http://scitation.aip.org/content/aip/journal/jcp/107/13?ver=pdfcov
Published by the AIP Publishing

Renner–Teller splitting in the C $1s\rightarrow\pi^*$ excited states of CS_2, OCS, and CO_2

Jun-ichi Adachi and Nobuhiro Kosugi[a)]
Institute for Molecular Science, Myodaiji, Okazaki 444, Japan

Eiji Shigemasa and Akira Yagishita
Photon Factory, National Laboratory for High Energy Physics, Tsukuba 305, Japan

(Received 16 May 1997; accepted 30 June 1997)

Fragment ions energetically emitted following the perpendicular ($\Delta\Lambda=+1$) transitions of C $1s\rightarrow\pi^*$ of CS_2, OCS, and CO_2 are observed not only in the perpendicular (90°) direction but also in the parallel (0°) to the linear polarization; that is, ions have a momentum orthogonal to the linear molecule. This arises in the Renner–Teller (RT) vibronic coupling of bending vibrations in the C $1s\rightarrow$ in-plane π^* excited state with a bent equilibrium geometry, though the RT splitting between the C $1s\rightarrow$ out-of-plane π^* state with a linear geometry and the C $1s\rightarrow$ in-plane π^* state is not visible directly due to the lifetime broadening. The 0° ion yield is relatively small in CS_2 but is comparable to the 90° yield in CO_2; in the latter the peak maximum at 0° is 0.06 eV lower than at 90° and the anisotropy parameter β is heavily dependent on the photon energy. In CO_2 a great number of unresolved bending vibrations are coupled. The half-width at half-maximum on the lower energy side of the π^* peak is much more sensitive to the RT splitting; 0.08, 0.11, and 0.29 eV for CS_2, OCS, and CO_2, compared with the full-width at half-maximum, 0.17, 0.39, and 0.64 eV. In CS_2 the π^* peak and β value are sharp and symmetric, indicating that the zero-point vibrational levels are only involved. In OCS three fine structures observed with separations of 0.21 eV are assigned to the ν_3 mode, which is comparable to the stretching mode in CO. © *1997 American Institute of Physics.* [S0021-9606(97)03137-1]

I. INTRODUCTION

Electronic structures and fragmentation dynamics of inner-shell excited states of some simple molecules are discussed by measuring the angular dependence of fragment ions using linearly polarized soft x rays.[1–22] In diatomic molecules[1–14] the fragment ions energetically emitted are detected in the parallel direction (0°) to the electric vector of the incident light for the parallel transition ($\Delta\Lambda=0$; for example, $1s\rightarrow\sigma^*$ excitation), and are detected in the perpendicular direction (90°) for the perpendicular transition ($\Delta\Lambda=\pm1$; for example, $1s\rightarrow\pi^*$ excitation).[7–11] This is rationalized by the axial recoil mechanism;[23,24] in the case of inner-shell excitation the ionic fragmentation following the Auger process takes place in a much shorter time than the period of the molecular rotation and the fragment ions emitted along repulsive potential energy curves have a memory of the molecular orientation and symmetry in the photoabsorption process.

On the other hand, for some linear triatomic molecules,[16–22] fragment ions energetically emitted are observed at 0° as well as at 90° in the core-to-π^* perpendicular ($\Delta\Lambda=+1$) transition.[19–22] That is, fragment ions with a momentum orthogonal to the linear molecular axis are emitted upon fragmentation following the Auger decay. The present authors have rationalized such incomplete $\Delta\Lambda=+1$ ''symmetry resolution'' in the core-to-π^* excited states of N_2O (Ref. 19) and CO_2 (Ref. 22) by the Renner–Teller effect. The twofold degeneracy of the core-to-π^* excited state is removed by the vibronic coupling with bending vibrations through the Renner–Teller effect and the core-to-π^* excited state is split into the core-to-$\pi^*_{\rm in}$ (in-plane π^*) and $\pi^*_{\rm out}$ (out-of-plane π^*) excited states with bent and linear equilibrium geometries, respectively, though the Renner–Teller splitting is not visible directly due to the lifetime broadening in inner-shell absorption spectroscopy. Thus, the vibronic coupling with bending vibrations is greatly enhanced through the Renner–Teller effect in the core-to-$\pi^*_{\rm in}$ excited state with a bent equilibrium geometry, and fragmentation from the core-to-$\pi^*_{\rm in}$ excited state results in the ion yields not only at 90° but also at 0°. In other words, the axial recoil mechanism fails when the bending vibration is highly excited and the anisotropy of the fragmentation following the inner-shell excitation should be related to the molecular vibration but not to the equilibrium geometry.[21,22]

In the present work, the Renner–Teller effect in the C $1s\rightarrow\pi^*$ excited state is investigated in detail by use of high-resolution angle-resolved ion-yield spectroscopy for linear triatomic molecules with a center carbon atom, CS_2, OCS, and CO_2. The present systematic study for the isoelectronic molecules reveals differences in strengths of the Renner–Teller effect related to the Renner–Teller splitting, vibrational modes coupled in the C $1s\rightarrow\pi^*$ excited states, and angular distributions of fragment ions.

a)Author to whom correspondence should be addressed.

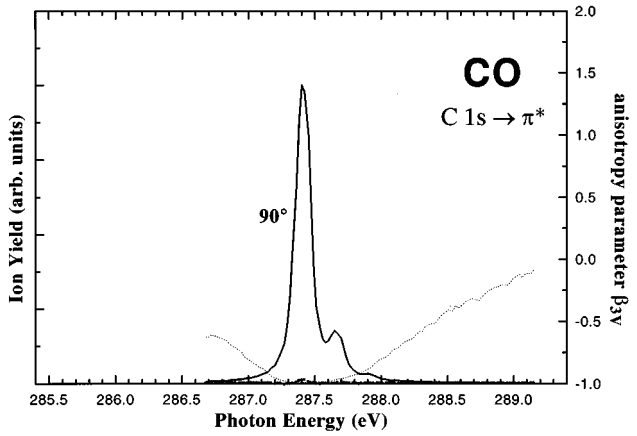

FIG. 1. Angle-resolved ion-yield spectra for the C $1s\rightarrow\pi^*$ excited state of CO measured with a bandpass of 0.08 eV and a retarding potential of $+3$ V applied. The solid line shows the ion yield measured at 90° and the dotted line at 0°, together with the anisotropy parameter β.

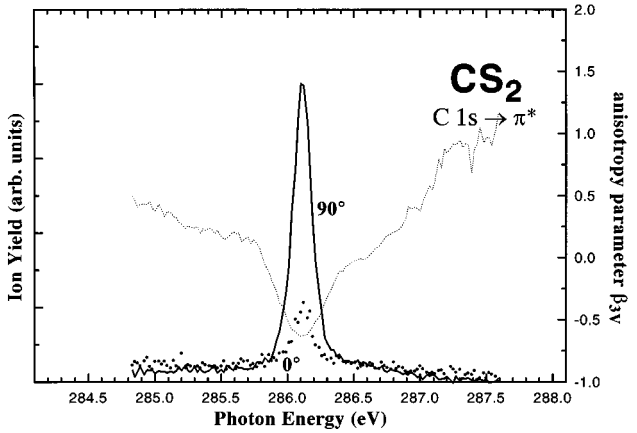

FIG. 2. Angle-resolved ion-yield spectra for the C $1s\rightarrow\pi^*$ excited state of CS_2 measured with a bandpass of 0.08 eV and a retarding potential of $+3$ V applied. The solid line shows the ion yield measured at 90° and the dotted line at 0°, together with the anisotropy parameter β.

II. METHODS

Experiments were carried out using a 10 m grazing-incidence monochromator installed at the soft x-ray undulator beamline BL-2B of the Photon Factory storage ring.[25] Fragment ions emitted from the interaction region of monochromatic light and sample gas were detected simultaneously using two channeltrons. The channeltrons were set on a plane perpendicular to the incident light and in the 0° (parallel) and 90° (perpendicular) directions relative to the electric vector of the linearly polarized light. The acceptance angle of the fragment ions in the detectors was limited to about $\pm 10°$ with the apertures of retardation electrodes, to which $+3$ V were applied; no thermal ion can reach the detector with the retardation fields.[14]

In the same experimental condition for CS_2, OCS, and CO_2, the C $1s$ photoabsorption spectra for CH_4 were obtained above the ionization threshold to calibrate the detection efficiencies of the two channeltrons.[4] This is reasonable because the angular distribution of the fragment ion is isotropic above the threshold in CH_4; on the other hand, the angular distribution is incompletely isotropic below the threshold even in CH_4 with an isotropic (T_d) geometry.[21] Furthermore, to correct imperfectness of linear polarization, which is caused by a tilted polarization plane, nonlinear polarization components, acceptance angle of the detectors, detection efficiencies, and other factors, the angle-resolved ion-yield spectra of CO were measured at the C $1s\rightarrow\pi^*$ excitation, because the ions should be observed only at 90°.[6] It was estimated that the spectrum observed at 0° involved about 20% of the spectrum observed at 90° (*vice versa*). In the following discussion, let the I_0 and I_{90} spectra denote the ion yields with the two channeltrons after normalization, background subtraction, and removal of imperfect polarization contribution. The photon-energy scale was calibrated using the C $1s\rightarrow 3s$ Rydberg peak at 292.74 eV on the basis of the high-resolution electron energy loss spectrum of CO_2.[26] In order to discuss the anisotropy on the emitted fragment ions, the anisotropy parameter $\beta_{3\,\mathrm{V}}$ obtained with the retarding potential of $+3$ V applied is defined as follows:[27]

$$\beta_{3\,\mathrm{V}}=\frac{2(I_0-I_{90})}{I_0+2\cdot I_{90}}.$$

III. RESULTS

Figure 1 shows the I_0 spectrum by using a dotted line and the I_{90} spectrum by a solid line for the C $1s\rightarrow\pi^*$ excited state of CO, for comparison with the triatomic molecules. A thin dotted line shows values of the anisotropy parameter $\beta_{3\,\mathrm{V}}$. As expected after the removal of imperfect polarization contributions, the I_0 spectrum is very weak and the $\beta_{3\,\mathrm{V}}$ is equal to -1 around the C $1s\rightarrow\pi^*$ peak maximum. The π^* peak in the I_{90} spectrum clearly shows three symmetric fine structures, which are attributed to three stretching vibrational levels, $v=0$, 1, and 2.[28] The full-width at half-maximum (FWHM) of the lowest fine structure in the I_{90} spectrum of CO is about 0.14 eV. Assuming that the shape of the monochromatic incident light is Gaussian and the lifetime width of the C $1s$ hole state of CO is 0.085 eV,[29] the bandpass of the incident light is estimated to be about 0.082 eV; that is, the energy resolution ($E/\Delta E$) is about 3500 in the present work.

Figures 2–4 show the I_{90} and I_0 spectra and the anisotropy parameter $\beta_{3\,\mathrm{V}}$ for the C $1s\rightarrow\pi^*$ excited states of CS_2, OCS, and CO_2 measured in the same experimental condition as the spectra of CO shown in Fig. 1. The 0° ion yield is very small in CS_2 and is comparable to the 90° ion yield in CO_2. The $\beta_{3\,\mathrm{V}}$ values on the π^* peak maximum in the I_{90} spectrum are -0.63 for CS_2, -0.42 for OCS, and -0.04 for CO_2, and the minimum $\beta_{3\,\mathrm{V}}$ values in a width of the π^* peak are -0.63 for CS_2, about -0.5 for OCS, and about -0.4 for CO_2. In CO_2 the $\beta_{3\,\mathrm{V}}$ values are heavily dependent on photon energies, and the peak maximum of the I_0 spectrum is 0.06 eV lower in energy than that of the I_{90} spectrum.

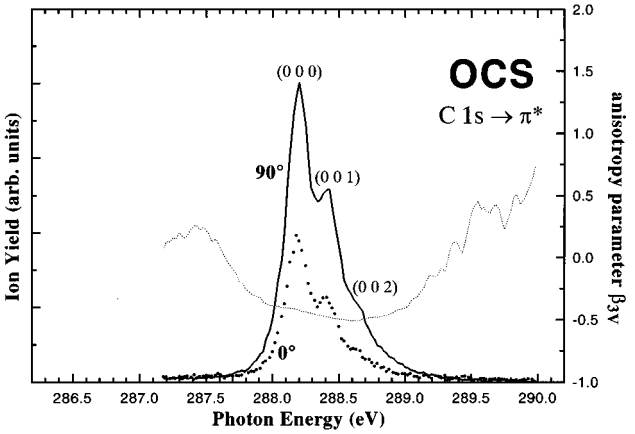

FIG. 3. Angle-resolved ion-yield spectra for the C $1s\rightarrow\pi^*$ excited state of OCS measured with a bandpass of 0.08 eV and a retarding potential of +3 V applied. The solid line shows the ion yield measured at 90° and the dotted line at 0°, together with the anisotropy parameter β.

The widths of the π^* peaks are larger for the triatomic molecules than for CO, but are rather dependent on the molecules. The width of the π^* peak of CS_2 shown in Fig. 2 is 0.17 eV in FWHM, which is slightly larger than that of CO, 0.14 eV, and is symmetric with no fine structure, where $HWHM_{lower}=HWHM_{higher}$ (half-width at half-maximum in the lower and higher energy sides)=0.08 eV. Wight and Brion[30] reported that the C $1s\rightarrow\pi^*$ peak in the electron energy-loss spectrum has a FWHM of 0.56 eV in comparison with the peak associated with elastically scattered electrons with a FWHM of 0.38 eV, and concluded that the π^* peak involves several vibrational levels. In disagreement with their observation and interpretation, the present high-resolution data indicate that the Renner–Teller splitting in the degenerate C $1s\rightarrow\pi^*$ excited states is less than 0.1 eV and the π^* peak in CS_2 corresponds only to zero-point vibrational levels (*vide infra*).

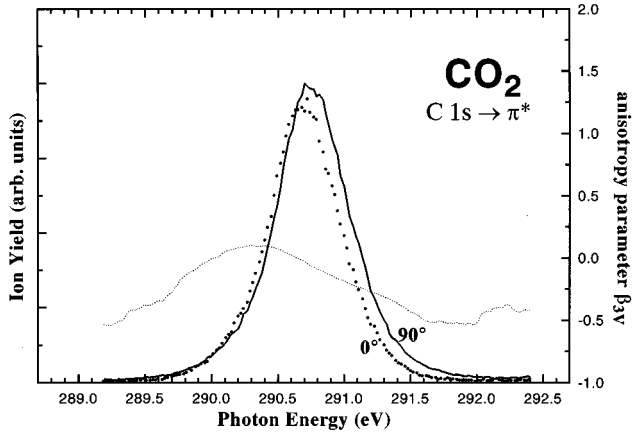

FIG. 4. Angle-resolved ion-yield spectra for the C $1s\rightarrow\pi^*$ excited state of CO_2 measured with a bandpass of 0.08 eV and a retarding potential of +3 V applied. The solid line shows the ion yield measured at 90° and the dotted line at 0°, together with the anisotropy parameter β.

On the other hand, as shown in Fig. 3 the π^* peak of OCS has three fine structures; two peaks and one shoulder, where $HWHM_{lower}=0.11$ eV for the lowest fine structure and the FWHMs for the fine structures are about 0.23 eV. The energy separation between the fine structures is 0.21 eV. The same fine structures were observed in the high-resolution electron energy loss spectrum by Tronc *et al.*,[26] though Wight and Brion[30] reported a single broad feature with a FWHM of 0.85 eV (elastic FWHM of 0.56 eV). Tronc *et al.* assigned them to asymmetric stretching vibrations $v=0$, 1, and 2.

Furthermore, the π^* peak of CO_2 is very broad with a FWHM of 0.64 eV and is asymmetric with HWHMs of 0.29 eV (lower) and 0.35 eV (higher). No fine structure is resolved even in the present high-resolution spectrum shown in Fig. 4 as observed in the moderate and high resolution electron energy loss spectra by Wight and Brion (the π^* peak with a FWHM of 0.9 eV)[31] and Tronc *et al.* (FWHM of 0.6 eV).[26] The π^* peak of CO_2 should involve much more vibronic levels than the π^* peaks of CS_2 and OCS.

IV. DISCUSSION

A. Vibrational fine structure

Triatomic molecules have three vibrational modes, ν_1, ν_2, and ν_3. In CS_2 and CO_2 with the $D_{\infty h}$ point group, the ν_1, ν_2, and ν_3 denote the symmetric stretching, bending, and antisymmetric stretching modes, respectively. In OCS with $C_{\infty v}$ point group, the ν_1, ν_2, and ν_3 modes correspond approximately to the C–S stretching, O–C–S bending, and C–O stretching modes, respectively, where the C–O stretching mode has a larger vibrational frequency than the C–S stretching mode.

Prior to discussion of molecular vibrations involved in the C $1s\rightarrow\pi^*$ peaks, we estimate vibrational frequencies in the C $1s\rightarrow\pi^*$ excited states of CS_2, OCS, and CO_2 based on the equivalent core model using their $Z+1$ analogs,[32] NS_2, ONS, and NO_2. The results are summarized in Table I. The degenerate C $1s\rightarrow\pi_u^*(\Pi_u)$ excited states of CS_2 and CO_2 are related to the ground states and Renner–Teller pair states of NS_2 and NO_2, where the ground states have a bent equilibrium geometry with an in-plane $\pi^*(a_1)$ electron and their Renner–Teller pair states have a linear equilibrium geometry with an out-of-plane $\pi^*(b_1)$ electron.[33] The spectroscopic constants of NS_2 have not been experimentally evaluated but are evaluated by *ab initio* quantum chemical calculations by Yamaguchi *et al.*[33] The spectroscopic constants of NO_2 in the ground state and some excited states are evaluated experimentally and theoretically.[34,35] Table I shows the vibrational frequencies in the C $1s\rightarrow\pi^*$ excited states of CS_2 and CO_2 which are estimated by using the theoretical constants of NS_2 (Ref. 33) and NO_2 (Ref. 34) after the mass correction. Differences in vibrational frequency between the ground state and the C $1s\rightarrow\pi^*$ excited state are at most 20% in CS_2 and CO_2. On the other hand, no spectroscopic constant of the $Z+1$ analog ONS is known experimentally or theoretically. The vibrational frequencies of OCS in the ground state are shown in Table I.[36] It is probable that the vibrational fre-

TABLE I. Molecular geometries, vibrational frequencies, and energy differences between Renner–Teller pair states estimated on the basis of the $Z+1$ analogy for the C $1s\rightarrow\pi^*$ excited states of CS_2, OCS, and CO_2.

	NS_2[a]		CS_2	NO_2[a,b]		CO_2	OCS
	calc.[c] A_1	calc.[c] B_1	expt.[d] ground	calc.[e] A_1	calc.[e] B_1	expt.[d] ground	expt.[d] ground
r_e (Å)	1.562	1.550	1.5526	1.195	1.202	1.1600	1.1543 (C–O) 1.5628 (C–S)
θ_e (deg.)	150.8	180.0	180.0	134.5	180.0	180.0	180.0
ν_1 (meV)	90.5	83.3	81.6	185.2	156.1	165.3	106.5
ν_2 (meV)	39.7[f]	47.4[f]	49.2	101.7[f]	⋯	82.7	64.5
ν_3 (meV)	171.7[f]	179.8[f]	190.3	239.5[f]	243.2[f]	291.7	255.6
ΔE (eV)	0.09			1.65			

[a]The results based on the double ζ basis set and singly and doubly configuration interaction (DZ-SDCI) calculations are cited to discuss NS_2 and NO_2 on the same level of approximation.
[b]The experimental r_e values are 1.1964 Å ($X\ ^2A_1$) and 1.23 Å ($1\ ^2B_1$), and the experimental θ_e value is 134.3° ($X\ ^2A_1$) (Ref. 40).
[c]Reference 33.
[d]Reference 36.
[e]Reference 34.
[f]Values after the mass correction.

quencies of the C $1s\rightarrow\pi^*$ excited state in OCS are in the same range of deviation from those of the ground state as in CS_2 and CO_2.

In the C $1s\rightarrow\pi^*$ excited states of CS_2, the estimated vibrational frequencies of the ν_1 symmetric mode (0.08 and 0.09 eV) and the ν_3 antisymmetric mode (0.16 and 0.17 eV) are comparable to or larger than the bandpass of the incident light (0.082 eV) and the lifetime width (at least 0.085 eV). If the π^* peak involved some ν_1 and/or ν_3 vibrational excitations in addition to the zero-point stretching vibrations, the π^* peak would be more or less asymmetric. Since the π^* peak observed in Fig. 2 is completely symmetric with the HWHM of 0.08 eV, the π^* peak involves only zero-point stretching vibrations. This is consistent with small difference in bond length (less than 0.01 Å) between the ground state and the C $1s\rightarrow\pi^*$ excited state as estimated in Table I. This implies that the π^* orbital ($3\pi_u$) of CS_2 is of little antibonding character.

On the other hand, the estimated vibrational frequency of the ν_2 bending mode in the C $1s\rightarrow\pi^*$ excited state of CS_2(0.04 eV) is smaller than the bandpass of the incident light and the lifetime width. If the stabilization energy from the linear to bent equilibrium geometry due to the Renner–Teller effect was rather larger than 0.1 eV, some ν_2 vibrational levels in the C $1s\rightarrow$in-plane π^* (π^*_{in}) excited state would be excited and the peak would have a tail on the lower energy side. This is in disagreement with the observation shown in Fig. 2 and with the small stabilization energy 0.09 eV estimated in Table I. Therefore, in CS_2 the stabilization energy, or Renner–Teller splitting between the C $1s\rightarrow\pi^*_{\text{in}}$ and C $1s\rightarrow\pi^*_{\text{out}}$ excited states, is smaller than the bandpass

TABLE II. Possible assignments of vibrational modes coupled, HWHMs on the lower and higher energy sides of the π^* peaks, Renner–Teller splittings, and antibonding characters in the C $1s\rightarrow$in-plane π^* (π^*_{in}) and out-of-plane π^* (π^*_{out}) excited states of CS_2, OCS, and CO_2.

Molecule	C $1s$ excited state	$(n_1n_2n_3)$[a]	$\text{HWHM}_{\text{lower}}$ (eV)	$\text{HWHM}_{\text{higher}}$ (eV)	Renner–Teller splitting	Antibonding character
CS_2	$a_1\ \pi^*_{\text{in}}$ $b_1\ \pi^*_{\text{out}}$	(0 0 0) (0 0 0)	0.08	0.08	small	weak
OCS	$a'\ \pi^*_{\text{in}}$ $a''\ \pi^*_{\text{out}}$	$(0\ j\ k)$[b] $(0\ 0\ k)$ $k=0,1,2$	0.11	0.28	medium	C–S weak C–O strong
CO_2	$a_1\ \pi^*_{\text{in}}$ $b_1\ \pi^*_{\text{out}}$	$(i\ j\ 0)$[b] $(i\ 0\ 0)$ $i=0,1,2$	0.29	0.35	large	strong

[a]The n_1, n_2, and n_3 correspond to the symmetric stretching, bending, and antisymmetric stretching modes in CS_2 and CO_2, respectively, and to the C–S stretching, O–C–S bending, and C–O stretching modes approximately in OCS, respectively.
[b]Vibrational frequencies of the bending modes are smaller than the lifetime widths; therefore, the assignment to singly isolated bending levels is not significant (Ref. 37).

of the incident light and the lifetime width. Thus, the π^* peak involves only zero-point stretching and bending vibrational levels in the C $1s\rightarrow\pi^*$ excited states with a small Renner–Teller splitting, as summarized in Table II.

In OCS, the spacing between the fine structures in the π^* peak, 0.21 eV, is relatively large. Considering that the ν_3 frequency in the π^* peak is at most 20% smaller than the ν_3 frequency in the ground state (0.26 eV) and is comparable to the stretching frequency in the C $1s\rightarrow\pi^*$ excitation in CO as shown in Fig. 1 (0.25 eV), the fine structures are undoubtedly attributable to the ν_3 vibrational mode (C–O stretching); that is, the three fine structures are assigned to the (0 0 0), (0 0 1), and (0 0 2) vibrational levels in the C $1s\rightarrow\pi^*$ excited states with a more or less Renner–Teller splitting as shown in Table II. The observation of distinct three ν_3 vibrational levels, which have a lower frequency than in the ground state, means that the equilibrium C–O distance changes greatly from that of the ground state and the π^* orbital is of C–O antibonding character. Furthermore, each fine structure seems to be asymmetric and slightly broader than the π^* features of CO and CS_2 as noticed by Tronc *et al.*;[26] for example, the $\mathrm{HWHM}_{\mathrm{lower}}$ of the lowest fine structure for OCS, 0.11 eV, is larger than 0.08 eV for CS_2. The fine structure in the π^* peak of OCS may involve some ν_1 (C–S stretching) or ν_2 (bending) vibrational levels in the C $1s\rightarrow\pi^*_{\mathrm{out}}$ and π^*_{in} excited states, where the frequencies are estimated to be less than 0.1 eV. Assuming that the C–S bond length in the C $1s\rightarrow\pi^*$ excited state of OCS is almost the same as in the ground state similarly to the case of CS_2, the ν_1 vibration is not coupled in the C $1s\rightarrow\pi^*$ excited state. Therefore, it is most probable that each fine structure involves some unresolved ν_2 levels in the C $1s\rightarrow\pi^*_{\mathrm{in}}$ excited state due to the Renner–Teller splitting as shown in Table II.

B. Line shape

The C $1s\rightarrow\pi^*$ excited state of CO_2 shows only a very broad peak with no fine structure. If the vibrational frequency is smaller than the lifetime width, the vibrational levels cannot be experimentally resolved and are no longer assigned to singly isolated vibronic levels as discussed by Neeb *et al.*[37] The most probable vibrations involved in the unresolved π^* peak of CO_2 are in the bending mode with a smaller frequency than the lifetime width and the bandpass of the incident light in the present experiment. To investigate unresolved vibrational levels, it is significant to discuss line shape and difference between the I_0 and I_{90} spectra as in the previous work on the O $1s\rightarrow\pi^*$ excitation of N_2O.[19] We discuss line shape in the I_{90} spectra in terms of $\mathrm{HWHM}_{\mathrm{lower}}$ and $\mathrm{HWHM}_{\mathrm{higher}}$ in this section, and difference between I_0 and I_{90} in terms of $\beta_{3\,\mathrm{V}}$ in the next section.

As shown in Fig. 5, the $\mathrm{HWHM}_{\mathrm{lower}}$ of the π^* peak originates only from bending vibrational levels in the C $1s\rightarrow\pi^*_{\mathrm{in}}$ excited state; on the other hand, the $\mathrm{HWHM}_{\mathrm{higher}}$ of the π^* peak is attributable to some vibronic levels both in the C $1s\rightarrow\pi^*_{\mathrm{in}}$ and π^*_{out} excited states, where the C $1s\rightarrow\pi^*_{\mathrm{in}}$ (in-plane π^* with a_1 or a' symmetry) and π^*_{out} (out-of-plane π^* with b_1 or a'' symmetry) excited states are produced

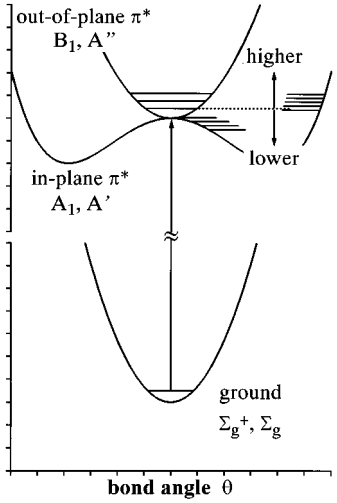

FIG. 5. Schematic representation of the potential energy curves as a function of the bending coordinate for the linear ground state, the bent C $1s\rightarrow$in-plane π^* (π^*_{in}) excited state, and the linear C $1s\rightarrow$out-of-plane π^* (π^*_{out}) excited state. The Franck–Condon factor for a linear-to-linear transition to the π^*_{out} state is much larger than for a linear-to-bent transition to the π^*_{in} state. The half-width at half-maximum (HWHM) on the lower energy side of the peak is related to the Renner–Teller splitting between the two excited states.

through the Renner–Teller coupling in the degenerate C $1s\rightarrow\pi^*$ excited state of linear triatomic molecules. Thus, the $\mathrm{HWHM}_{\mathrm{lower}}$ is related to the Renner–Teller splitting between the C $1s\rightarrow\pi^*_{\mathrm{in}}$ and π^*_{out} excited states, though the lifetime width and the bandpass of the incident light contribute to the HWHM as well. In other words, as discussed by Tronc *et al.*,[26] the π^* peak is caused by transitions to high bending levels of the C $1s\rightarrow\pi^*_{\mathrm{in}}$ excited state with $^1A_1$ or $^1A'$ symmetry on the lower energy side of the peak and to some vibrational levels of the C $1s\rightarrow\pi^*_{\mathrm{out}}$ excited state with $^1B_1$ or $^1A''$ symmetry on the higher energy side. It should be noticed that the Franck–Condon factor along the bending coordinate is larger in linear-to-linear transitions to the C $1s\rightarrow\pi^*_{\mathrm{out}}$ excited state than in linear-to-bent ones to the C $1s\rightarrow\pi^*_{\mathrm{in}}$ excited state as discussed by Wight and Brion.[31]

The $\mathrm{HWHM}_{\mathrm{lower}}$ in the π^* peak at 90° of CO_2, 0.29 eV, is much larger than the $\mathrm{HWHM}_{\mathrm{lower}}$ for OCS (0.11 eV) and CS_2 (0.08 eV). This result indicates that the Renner–Teller splitting is much larger in CO_2 than in CS_2 and OCS. This is reasonable, considering that the stabilization energy from the linear to bent equilibrium geometry based on the $Z+1$ analogy is the largest in CO_2 (1.65 eV) and the bent equilibrium geometry is most greatly distorted from linear ($\theta=135°$). The $\mathrm{HWHM}_{\mathrm{lower}}$ of the π^* peak for CO_2 is much smaller than the stabilization energy, because transitions to a number of low-lying vibrational levels around a bent equilibrium geometry in the C $1s\rightarrow\pi^*_{\mathrm{in}}$ excited state are almost forbidden from the ground state with a linear equilibrium geometry.

The $\mathrm{HWHM}_{\mathrm{higher}}$ of 0.35 eV is larger than the $\mathrm{HWHM}_{\mathrm{lower}}$ of 0.29 eV in the π^* peak at 90° for CO_2. The higher energy side of the π^* peak may involve some ν_1 (symmetric) or ν_3 (antisymmetric) stretching vibrations in

the C $1s\rightarrow\pi^*_{out}$ and π^*_{in} excited states in addition to the ν_2 bending vibrations in the C $1s\rightarrow\pi^*_{in}$ excited state due to the Renner–Teller splitting. This is consistent with large difference in bond length (more than 0.03 Å) between the ground state and the C $1s\rightarrow\pi^*$ excited states, based on the $Z+1$ analogy as shown in Table I, and with antibonding character of the π^* orbital ($2\pi_u$) of CO_2. However, the transition to the ν_3 vibrational levels is almost forbidden in CO_2, because the plane symmetry with equal C–O bond lengths is retained in the C $1s\rightarrow\pi^*$ excited state as well as in the ground state and the transitions to the antisymmetric stretching vibrations with odd quantum numbers are forbidden. Thus, the π^* peak of CO_2 involves some ν_1 vibrations; probably, $v=0$, 1, and 2, considering the $HWHM_{higher}$ of 0.35 eV and the ν_1 vibrational frequencies of 0.16–0.19 eV as shown in Table I, which are larger than the bandpass of the incident light and the lifetime width. No fine structure is resolved in the ν_1 vibrational mode, because a great number of unresolved ν_2 bending vibrations in the C $1s\rightarrow\pi^*_{in}$ excited state due to a relatively large Renner–Teller splitting have a band width comparable to the $HWHM_{lower}$ of 0.29 eV, and partly because the ν_1 vibrational frequencies are different in the C $1s\rightarrow\pi^*_{out}$ and π^*_{in} excited states. A possible assignment of the vibrational levels involved in the π^* peak of CO_2 is shown in Table II.

C. Angular distribution of fragment ions

In CO_2 the $\beta_{3\nu}$ value shows strong energy dependence within a broad peak width from 0 to -0.4, and the π^* peak of CO_2 shows a different feature between the I_{90} and I_0 spectra; difference in energy between the I_{90} and I_0 peak maxima is 0.06 eV. A similar energy dependence of the fragment ion yields has already been observed for the O $1s\rightarrow\pi^*$ excited state in N_2O, where the difference in peak maximum is 0.17 eV;[19] furthermore, the I_{90} and I_0 ion yields show different vibronic couplings in the C $1s\rightarrow 3pt_2$ Rydberg excitation of CH_4 (Ref. 21) and the C $1s\rightarrow 4s$ Rydberg transitions of CO_2.[22] The present result can be explained by assuming a large Renner–Teller splitting in the C $1s\rightarrow\pi^*$ excited state in CO_2 as well as in the O $1s\rightarrow\pi^*$ excited state in N_2O. As shown in Fig. 6, the Renner–Teller splitting is dependent on strength of the Renner–Teller coupling. In the case of the strong Renner–Teller effect as in CO_2, the bending mode is highly excited in the C $1s\rightarrow\pi^*_{in}$ excited state. Therefore, on the lower energy side the angular dependence of total fragment ion yields is almost isotropic ($\beta_{3\,V}\sim 0$); on the higher energy side the transition probability to the C $1s\rightarrow\pi^*_{out}$ excited state with a linear equilibrium geometry is dominant, and the anisotropy parameter $\beta_{3\,V}$ decreases its value toward -1. At the present stage of study it seems to be difficult to discuss the relationship between the anisotropy parameter β and the fragmentation mechanism in detail. For example, Wight and Brion[31] reported that the core-to-π^* excited state decays through the Auger emission in a much shorter time than that required for a molecular vibration and the excited molecule does not reach the bent equilibrium conformation; on the other hand, Neeb *et al.*[37] have recently

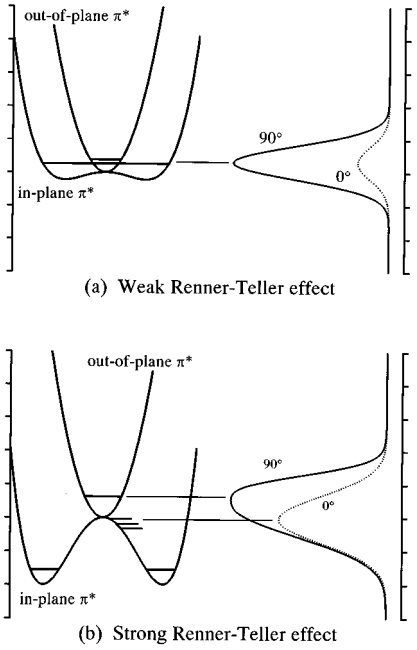

FIG. 6. Schematic potential energy curves of the C $1s\rightarrow$in-plane π^* (π^*_{in}) and out-of-plane π^* (π^*_{out}) excited states for the two extreme cases, (a) weak and (b) strong Renner–Teller effects. The thick lines indicate the zero-point bending vibrations. The C $1s\rightarrow\pi^*_{in}$ excited state is vibronically coupled with bending vibrations through the Renner–Teller effect, and results in the fragmentation in both the 90° and 0° directions; on the other hand, the C $1s\rightarrow\pi^*_{out}$ excited state is not coupled with bending vibrations, and results in the fragmentation only in the 90° direction. In other words, the 90° ion yield arises from both C $1s\rightarrow\pi^*_{in}$ and π^*_{out}, and the 0° yield only from C $1s\rightarrow\pi^*_{in}$. To compare with experimental ion yields, the stretching vibrations, the lifetime broadening, and the bandpass of the incident light should be taken into account.

discussed a possibility that the Auger decay occurs at classical turning points on the potential energy curve. Furthermore, it is noticed that the anisotropy parameter β is dependent on both kinetic energies and species of fragment ions.[18–20] In any case, it is of no significance to relate the β value directly to a unique bond angle in the C $1s\rightarrow\pi^*$ excited state, which is strongly coupled with bending motions and is split into the C $1s\rightarrow\pi^*_{in}$ and π^*_{out} states through the Renner–Teller effect, though the Renner–Teller splitting is not visible directly due to the lifetime broadening.

In the case of the weak Renner–Teller effect as in CS_2 and OCS, the Renner–Teller splitting is comparable to the lifetime width and the bending mode is not so much excited in the C $1s\rightarrow\pi^*_{in}$ excited state; the I_0 spectrum is almost proportional to the I_{90} spectrum and the $\beta_{3\,V}$ value is not so far from -1 as shown in Fig. 6. There is no energy difference between the I_0 and I_{90} peak maxima in CS_2 and OCS; therefore, the energy difference in peak maximum is less sensitive to the Renner–Teller splitting than the HWHM on the lower energy side of the peak. It is interesting that the anisotropy parameter $\beta_{3\,V}$ in OCS (Fig. 3) slightly decreases as the incident photon energy increases from the (0 0 0) level at 288.2 eV to the (0 0 2) level at 288.67 eV. This implies that each ν_3 vibrational level is more or less coupled with

bending vibrations in the C $1s\rightarrow\pi^*_{in}$ excited state of OCS as shown in Table II.

The anisotropy parameter $\beta_{3\,V}$ in CS_2 (Fig. 2) shows a symmetric curve within the π^* peak width and has small values of $-0.5\sim-0.6$. This supports the above interpretation in terms of HWHM that the π^* peak involves only zero-point stretching and bending vibrations in the C $1s\rightarrow\pi^*_{out}$ and π^*_{in} excited states of CS_2 as shown in Table II. Hayes[38] measured the mass-selected ion-yield spectra for CS_2 in the C 1*s* and S 2*p* excited regions, and found fragment ions with $m/e=64$ at the C $1s\rightarrow\pi^*$ excitation. The $m/e=64$ fragments are due to the S_2^+ ions; that is, the rearrangement of the chemical bond occurs following the Auger decay from the C $1s\rightarrow\pi^*$ excited state. Although no species arising from the rearrangement of the chemical bond such as S_2^+ is observed in N_2O (Ref. 16) and CO_2,[39] his observation is not inconsistent with the present interpretation of the vibronic levels in the C $1s\rightarrow\pi^*$ excited state, considering that the bending vibrational period is comparable to the lifetime of the C 1*s* vacancy and the molecule may have a momentum orthogonal to the linear axis upon fragmentation following the Auger decay from excited states, in particular the C $1s\rightarrow\pi^*_{in}$ excited state, with zero-point bending vibrations.[20,22] If the production rate of the S_2^+ fragments is faster than the molecular rotation, the S_2^+ fragment ions will be observed mainly in the 0° direction, similarly to the C^+ ions emitted from the C $1s\rightarrow\pi^*$ excitation of CO_2.[18]

V. SUMMARY

The high-resolution angle-resolved ion-yield spectra with a bandpass of 0.08 eV were measured for the C $1s\rightarrow\pi^*$ transitions of CS_2, OCS, and CO_2, where the lifetime of the C $1s\rightarrow\pi^*$ excited states is expected to be comparable to that in CO (0.085 eV). The FWHMs of the π^* peaks are 0.17, 0.39, and 0.64 eV for CS_2, OCS, and CO_2, respectively, compared with the FWHM of 0.14 eV for a single vibrational level in the C $1s\rightarrow\pi^*$ transition of CO. The $HWHM_{lower}$ of the π^* peaks are 0.08, 0.11, and 0.29 eV; the π^* peak is asymmetric in OCS and CO_2. The symmetric and sharp π^* peak of CS_2 indicates that the Renner–Teller splitting between the C $1s\rightarrow\pi^*_{in}$ excited state with a bent equilibrium geometry and the C $1s\rightarrow\pi^*_{out}$ excited state with a linear equilibrium geometry is less than 0.1 eV and the zero-point stretching and bending vibrational levels are only involved in the peak. On the other hand, the Renner–Teller splitting is very large for CO_2, and a great number of unresolved vibrational levels of the bending and symmetric stretching modes are coupled in the C $1s\rightarrow\pi^*_{in}$ and π^*_{out} excited states. For OCS the three fine structures observed with separations of 0.21 eV are assigned to $v=0$, 1 and 2 of the ν_3 C–O stretching mode involving some bending vibrations in the C $1s\rightarrow\pi^*_{in}$ excited state. Possible vibrational modes in the C $1s\rightarrow\pi^*$ excited states are summarized in Table II.

Fragment ions are energetically emitted not only in the 90° direction but also in the 0° direction in the C $1s\rightarrow\pi^*$ excitation; the $\beta_{3\,V}$ values observed at the peak maxima are -0.63, -0.42, and -0.04 for CS_2, OCS, and CO_2, respectively. That is, fragment ions with a momentum orthogonal to the linear molecular axis are emitted upon fragmentation following the Auger decay. This is related to strong vibronic coupling of the C $1s\rightarrow\pi^*_{in}$ excited state with bending vibrations through the Renner–Teller effect. In the case of the strong Renner–Teller effect as in CO_2, the 0° ion yield is comparable to the 90° ion yield; that is, fragmentation is almost isotropic. Furthermore, the peak maximum in the I_0 spectrum of CO_2 is 0.06 eV lower in energy than that in the I_{90} spectrum and the $\beta_{3\,V}$ values are heavily dependent on photon energies within the peak width. Similar behaviors have already been observed for the O $1s\rightarrow\pi^*$ excitation with the Renner–Teller vibronic coupling in N_2O,[19] the C $1s\rightarrow 3pt_2$ Rydberg excitation with the Jahn–Teller vibronic coupling in CH_4,[21] and the vibronically-induced C $1s\rightarrow 4s$ Rydberg excitation of CO_2.[22] The angle-resolved ion-yield technique is very powerful for elucidating various types of vibronic couplings in inner-shell excited states.

ACKNOWLEDGMENTS

The present authors are grateful to the staff of the Photon Factory for the stable operation of the storage ring. The present work has been performed under approval of the Photon Factory Committee (Proposal No. 92G-142).

[1] N. Saito and I. H. Suzuki, Phys, Rev. Lett. **61**, 2740 (1988); J. Phys. B **22**, 3973, L517 (1989).
[2] A. Yagishita, H. Maezawa, M. Ukai, and E. Shigemasa, Phys. Rev. Lett. **62**, 36 (1989).
[3] E. Shigemasa, K. Ueda, Y. Sato, T. Hayaishi, H. Maezawa, T. Sasaki, and A. Yagishita, Phys. Scr. **41**, 63 (1990).
[4] K. Lee, D. Y. Kim, C. I. Ma, D. A. Lapiano-Smith, and D. M. Hanson, J. Chem. Phys. **93**, 7936 (1990).
[5] N. Saito and I. H. Suzuki, Phys. Rev. A **43**, 3662 (1991).
[6] E. Shigemasa, K. Ueda, Y. Sato, T. Sasaki, and A. Yagishita, Phys. Rev. A **45**, 2915 (1992).
[7] N. Kosugi, E. Shigemasa, and A. Yagishita, Chem. Phys. Lett. **190**, 481 (1992).
[8] N. Kosugi, J. Adachi, E. Shigemasa, and A. Yagishita, J. Chem. Phys. **97**, 8842 (1992).
[9] A. Yagishita, E. Shigemasa, J. Adachi, and N. Kosugi, in *Vacuum Ultraviolet Radiation Physics*, in *Proceedings of the 10th VUV Conference*, edited by F. J. Wuilleumier, Y. Petroff, and I. Nenner (World Scientific, Singapore, 1993), p. 201.
[10] A. Yagishita and E. Shigemasa, Rev. Sci. Instrum. **63**, 1383 (1992).
[11] E. Shigemasa, T. Hayaishi, T. Sasaki, and A. Yagishita, Phys. Rev. A **47**, 1824 (1993).
[12] J. D. Bozek, N. Saito, and I. H. Suzuki, J. Chem. Phys. **100**, 393 (1994).
[13] K. Lee, D. Y. Kim, C. I. Ma, and D. M. Hanson, J. Chem. Phys. **100**, 8550 (1994).
[14] A. Yagishita, E. Shigemasa, and N. Kosugi, Phys. Rev. Lett. **72**, 3961 (1994).
[15] D. Y. Kim, K. Lee, C. I. Ma, M. Mahalingam, D. M. Hanson, and S. L. Hulbert, J. Chem. Phys. **97**, 5915 (1992).
[16] T. LeBrun, M. Lavollée, M. Simon, and P. Morin, J. Chem. Phys. **98**, 2534 (1993).
[17] J. D. Bozek, N. Saito, and I. H. Suzuki, J. Chem. Phys. **98**, 4652 (1993).
[18] J. D. Bozek, N. Saito, and I. H. Suzuki, Phys. Rev. A **51**, 4563 (1995).
[19] J. Adachi, N. Kosugi, E. Shigemasa, and A. Yagishita, J. Chem. Phys. **102**, 7369 (1995).
[20] J. Adachi, N. Kosugi, E. Shigemasa, A. Yagishita, and P. A. Hatherly, J. Electron Spectrosc. **79**, 491 (1996).
[21] N. Kosugi, J. Electron Spectrosc. **79**, 351 (1996).
[22] J. Adachi, N. Kosugi, E. Shigemasa, and A. Yagishita, J. Phys. Chem. **100**, 19 783 (1996).
[23] R. N. Zare, Mol. Photochem. **4**, 1 (1972).

[24] G. E. Busch and K. R. Wilson, J. Chem. Phys. **56**, 3638 (1972).
[25] A. Yagishita, S. Masui, T. Toyoshima, H. Maezawa, and E. Shigemasa, Rev. Sci. Instrum. **63**, 1351 (1992).
[26] M. Tronc, G. C. King, and F. H. Read, J. Phys. B **12**, 137 (1979).
[27] The present anisotropy parameter is a phenomenological one and is not directly related to the asymmetry parameter β defined by $2 \cdot P_2(\cos \chi)$, where P_2 is the second Lagendre polynomial function and χ is the angle between the broken bond on fragmentation and the vector of transition dipole moment for photoexcitation.
[28] J. T. Francis, N. Kosugi, and A. P. Hitchcock, J. Chem. Phys. **101**, 10 429 (1994).
[29] M. Coville and T. D. Thomas, Phys. Rev. A **43**, 6053 (1991).
[30] G. R. Wight and C. E. Brion, J. Electron Spectrosc. **4**, 335 (1974).
[31] G. R. Wight and C. E. Brion, J. Electron Spectrosc. **3**, 191 (1974).
[32] W. H. E. Schwarz, Angew. Chem. Int. Ed. **13**, 454 (1974).
[33] Y. Yamaguchi, Y. Xie, R. S. Grev, and H. F. Schaefer III, J. Chem. Phys. **92**, 3683 (1990); Y. Yamaguchi, Y. Xie, I. L. Alberts, R. S. Grev, and H. F. Schaefer III, *ibid*. **93**, 5053 (1990).
[34] Y. Xie, R. D. Davy, B. F. Yates, C. P. Blahous, Y. Yamaguchi, and H. F. Schaefer III, Chem. Phys. **135**, 179 (1989); C. P. Blahous, B. F. Yates, Y. Xie, and H. F. Schaefer III, J. Chem. Phys. **93**, 8105 (1990).
[35] C. F. Jackels and E. R. Davidson, J. Chem. Phys. **64**, 2908 (1976).
[36] G. Herzberg, *Molecular Spectra and Molecular Structure* (Van Nostrand, Princeton, NJ, 1967), Vol. III.
[37] M. Neeb, J.-E. Rubensson, M. Biermann, and W. Eberhardt, J. Electron Spectrosc. **67**, 261 (1994).
[38] R. G. Hayes, J. Chem. Phys. **86**, 1683 (1987).
[39] A. P. Hitchcock, C. E. Brion, and M. J. van der Wiel, Chem. Phys. Lett. **66**, 213 (1979).
[40] J. H. Callomon, E. Hirota, T. Iijima, K. Kuchitsu, and W. J. Lafferty, *Landolt–Börnstein New Series*, *Structure Data of Free Polyatomic Molecules* (Springer, Berlin, 1987), Vol. II/15.